

Integrating PS-InSAR and SBAS-InSAR for mining surface settlement monitoring

Based on 38 Sentinel-1A images, this paper imports GCP points generated by PS-InSAR into SBAS-InSAR, instead of manually selected GCP points, extracts surface deformation in the study area, and compares and analyzes with traditional GPS monitoring data. The results show that during the study period, obvious settlement funnels appeared in the southern and eastern parts of the study area. The maximum settlement along the line of sight reached 66mm, and the maximum settlement rate was -53mm/a, and the settlement results of InSAR are consistent with GPS monitoring results. The consistency verifies the feasibility of integrating InSAR technology to monitor surface subsidence in mining areas.

Keywords: Fusion; PS-InSAR; SBAS-InSAR; mining area; land subsidence

1.0 Introduction

Mining in mining areas often causes a series of geological disasters such as ground subsidence and subsidence, which seriously threaten the lives and property safety of people in and around the mining area. Monitoring the settlement of the mining area is an important task in the mining process, and how to monitor the settlement of the mining area quickly and effectively has important research significance. Traditional methods commonly used for surface subsidence monitoring, such as GPS monitoring, leveling, etc., are difficult to meet the real-time monitoring of small deformations in large areas due to their huge workload.

With the advancement of science and technology, there are also new methods for monitoring surface subsidence in mining areas. Synthetic Aperture Radar Interferometric (InSAR) technology has been increasingly used in mining surface settlement monitoring due to its high precision and high timeliness. The Small Baseline Subset technology (SBAS-InSAR) technology has the characteristics of mitigating the effects of time-space miscorrelation and

atmospheric delay. It can monitor small surface deformations for a long time and obtain more reliable monitoring results. Xu Jun [1] et al. used SBAS-InSAR technology to monitor the surface settlement of villages around the mining area based on 31 Sentinel-1A images, and compared to the measured data. The results showed that the use of SBAS-InSAR technology to monitor the surface settlement caused by mining in the mining area is Reliable; Zhou Wentao [2] and others imported the SBAS-InASR monitoring results into the combined model of the differential integrated moving average autoregressive model and the exponential smoothing model to monitor the surface subsidence of the mining area. The results show that the SBAS-InSAR monitoring value is the actual value The prediction results of has higher accuracy and higher timeliness.

When refining the orbit, the more stable the introduced ground control point (GCP), the better the elimination of the leveling effect. However, when SBAS-InSAR selects GCP points, it is difficult to find enough GCP points, and it is impossible to establish a large number of artificially stable targets, which leads to excessive manual intervention in the SBAS process and the possibility of introducing errors. In turn, the interference result does not meet the standard, and there is not enough deformation information. In view of the fact that SBAS-InSAR uses manual acquisition of GCP points in the step of orbit refining and re-leveling, the artificial introduction of large errors, while the permanent scatter radar interferometry (PS-InSAR) technology sets the amplitude dispersion threshold and coherence Threshold and spatial and low-pass filtering, time threshold high-pass filtering, reduce the atmospheric delay phase error in the interference phase to obtain more stable deformation information, and finally through coordinate transformation, it can be converted into a more stable GCP point in the SBAS process. Therefore, this article combines the advantages of PS-InSAR technology [3], the GCP points automatically collected by the software in the PS-InSAR process are used as the control points of SBAS-InSAR for orbit refining and re-leveling to reduce errors caused by human interference. Conduct surface settlement monitoring in the study area.

Blind peer reviews carried out

Messrs. Yang Yuan-ji, Zhang Wen-jun, Geng Shi-hua, Miao Jun-yi and Shen Rui, School of Environment and Resources, Southwest University of Science and Technology, Mianyang S&T City Division National Remote Sensing Center of China, Mianyang, Sichuan, China 621010

2.0 Overview of the study area and data sources

This article takes the second mining area of the Longshou mine in Jinchang City, Gansu Province, China as the research area (the second mining area for short). The location of the study area is shown in Fig.1. The mining area is flat, with an average altitude of 1500~1800m. The mining area has a dry climate and an undeveloped water system. It has a temperate continental climate. Due to long-term mining, the surface subsidence and settlement are serious, and the cracks are obvious, which poses a serious threat to safety production.



Fig.1: Location of the study area

Select Sentinel-1A continuous 38 scenes C-band ascending slant distance single-look complex (SLC) SAR images from 2019-03-22~2020-06-08, with a period of 12d and a resolution of 5m×20m. The detailed parameters are shown in the Table 1. Select the SRTM-DEM data with a resolution of 30m as the reference DEM.

TABLE 1: IMAGE DATA PARAMETERS

Parameter	Sentinel-1A	parameter	Sentinel-1A
Track configuration	Ascending	wavelength/cm	5.6
Imaging mode	IW	cycle/d	12
Polarization mode	VV	Angle of incidence/(°)	39.2
bandwidth	250	Ground resolution/m	30

3.0 Technical principle

3.1 PS-InSAR TECHNOLOGY PRINCIPLE

PS-InSAR technology uses multiple SAR images covering the same area to generate time-series interference image pairs through statistical analysis of the image amplitude information, and extract permanent scatterer points that are not affected by time-space baseline miscorrelation and atmospheric effects. Finally, the topographic phases on these target points are separated to monitor surface subsidence. [4-9]

Assuming that SLC images of different periods of M+1 scene in the unified study area are obtained, the main image

is selected based on the Doppler centroid frequency and time baseline, and the remaining M scene images are auxiliary images. The main images are matched with the auxiliary images. Alignment and interference processing, and then introduce DEM to remove the topographic phase, and generate the interferogram after the flattening effect and the topographic effect. Among them, the differential phase corresponding to each pixel is represented by formula (1).

$$\varphi = \varphi_{def} + \varphi_{topo} + \varphi_{atm} + \varphi_{orb} + \varphi_{noi} \quad \dots (1)$$

Where: φ is the differential phase of each pixel; φ_{def} is the deformation phase; φ_{topo} is the terrain phase; φ_{atm} is the atmospheric phase; φ_{orb} is the orbit error phase; φ_{noi} is the noise phase. Among them, can be eliminated by introducing AUX_POEORB precise orbit determination ephemeris data during data preprocessing, while and are caused by DEM accuracy problems and atmospheric delay.

2.2 SBAS-IN SAR TECHNOLOGY PRINCIPLE

SBAS technology is a new timing InSAR technology proposed by Berardinno et al. in 2002 in order to reduce space and time decoherence [10~12]. The principle is:

Assuming that N SAR image data of the study area composed of time series composed of $t_0, t_1 \dots t_n$, time and space baseline thresholds are set, combined with interference conditions, the images are subjected to differential interference processing to obtain M interference fringe patterns. Where M can be expressed as:

$$\frac{N}{2} \leq M \leq \frac{N(N-1)}{2} \quad \dots (2)$$

Set t_0 as the initial moment, then the phase difference at other moments t_i ($i = 1, 2, \dots, N$) is $\phi(t_i)$. After removing the flat-ground phase, the interference phase expression of the xth pixel of the kth interferogram is:

$$\delta\phi_{x,k} = \phi_{x,k}(t_B) - \phi_{x,k}(t_A) \approx \delta\phi_{def,x,k} + \delta\phi_{e,x,k} + \delta\phi_{a,x,k} + \delta\phi_{n,x,k} \quad \dots (3)$$

In the above formula: t_A, t_B ($t_A < t_B$) are the corresponding SAR image acquisition moments; $\delta\phi_{def,x,k}$ is the deformation phase in the line of sight; $\delta\phi_{e,x,k}$ is Terrain phase error; $\delta\phi_{a,x,k}$ is the atmospheric phase error; $\delta\phi_{n,x,k}$ is the noise phase error.

Deformation phase can be expressed by equation (4):

$$\delta\phi_{def,x,k} = \frac{4\pi}{\lambda} [d_{x,k}(t_B) - d_{x,k}t_A] \quad \dots (4)$$

In the formula: λ is the radar wavelength;

After removing the influence of terrain, atmosphere, and noise, the expression of interference phase is simplified to:

$$\delta\phi_{x,k} = \phi_{x,k}(t_B) - \phi_{x,k}(t_A) \approx \frac{4\pi}{\lambda} [d_{x,k}(t_B) - d_{x,k}(t_A)] \quad \dots (5)$$

The above formula can be rewritten into a matrix form as:

$$\delta\phi = A\phi \quad \dots (6)$$

In the above formula, A is an $M \times N$ matrix.

Finally, the singular value decomposition method is used to jointly solve multiple small baseline sets, and then the least

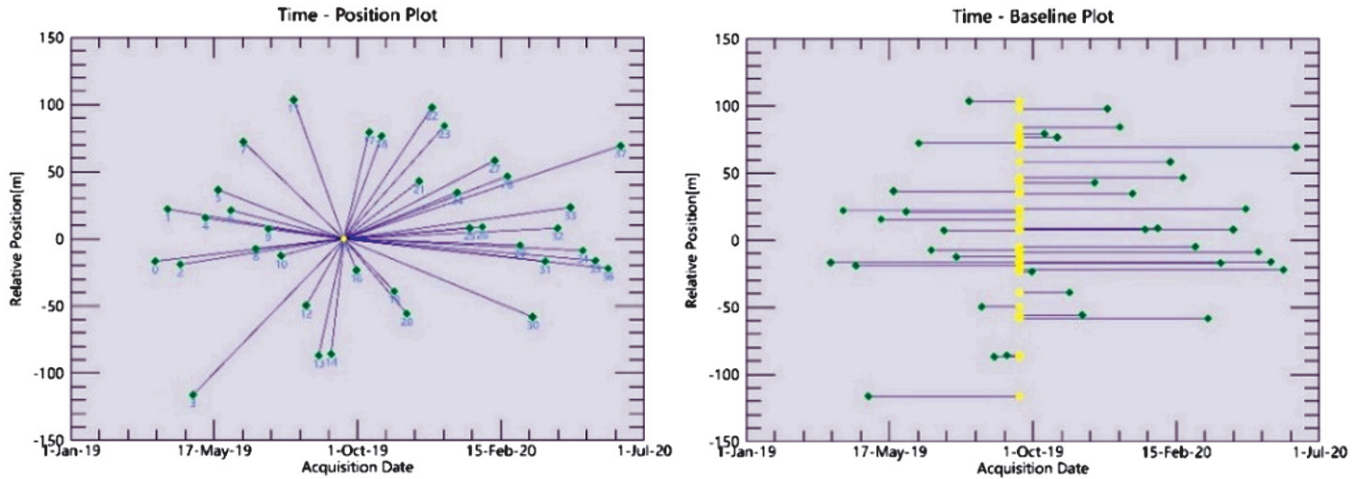


Fig.2: The space/time baseline situation of the image pair connection

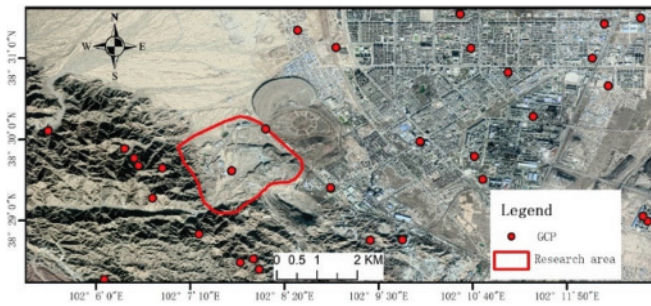


Fig.3: GCP points

square solution in the sense of the smallest norm of the cumulative deformation variable is obtained, and the deformation variable is estimated.

4.0 Data processing

4.1 PS-IN SAR PROCESSING

SARscape software is used for PS-InSAR data processing. First, the software automatically selects a super master image, and establishes a master-slave data pair for other data and the super master image according to the set critical baseline threshold, and the space/time baseline connection of the generated image pair connection is shown in Fig.2. After that, the master-slave image registration, interferogram generation, external DEM data is introduced to flatten the interference phase, and the amplitude dispersion index is calculated. After the first inversion of PS, the displacement rate and residual topography are obtained, which are used to flatten the synthesized interferogram. In this step, the GCP selected in the slope distance geometry and the GCP converted into geographic coordinates will be obtained. After the second inversion of PS, the atmospheric phase component is estimated, and the

atmospheric phase component is removed to obtain the final deformation rate. Finally, geocoding is performed to obtain the GCP points of PS-InSAR in geographic coordinates, as shown in Fig.3, as well as the cumulative deformation and deformation rate in geographic coordinates.

4.2 SBAS-IN SAR PROCESSING

SBAS-InSAR is also carried out in the SARscape software, and the key steps of data processing are shown in Fig.4. First, the data is paired with interference pairs, and the space/time baseline of the pair connection is generated by setting the time and space thresholds as shown in Fig.5. Then, the external DEM data is used to perform differential interference processing on the interference pair, and the Goldstein method is used for adaptive filtering and the

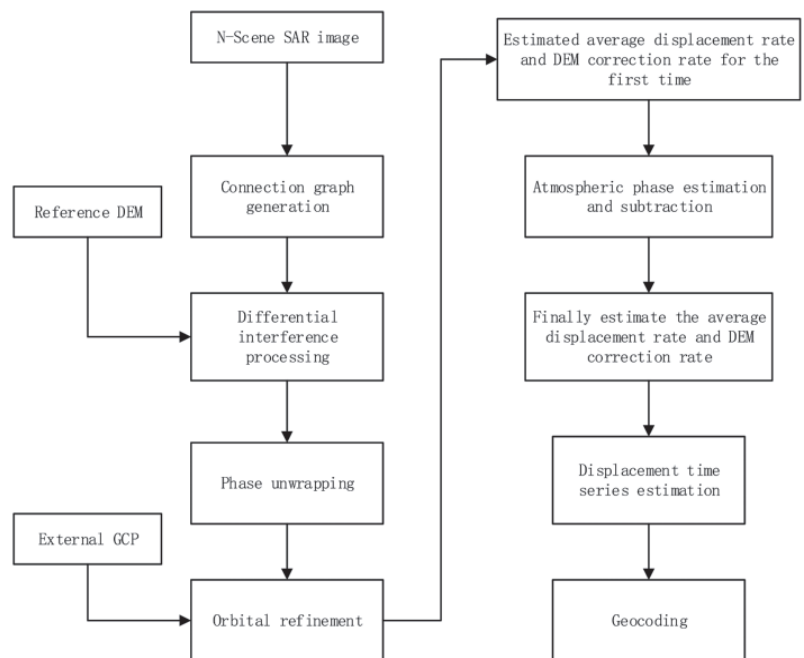


Fig.4 Flowchart of SBAS method

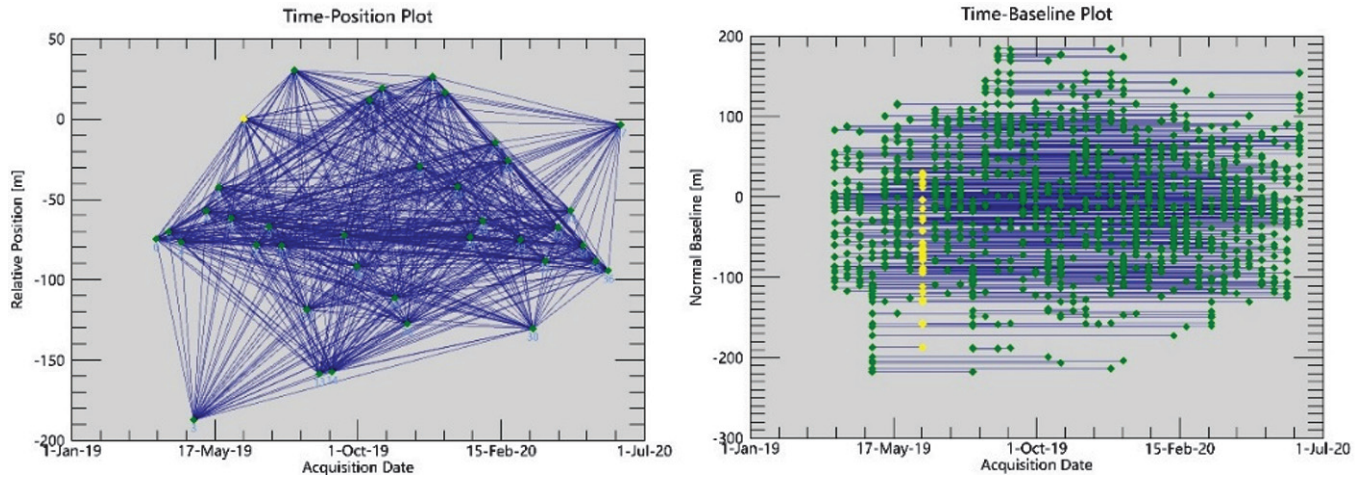


Fig.5: Space/time baseline situation of SBAS-InSAR image pair connection

minimum cost flow method for phase unwrapping.

Next, the geocoded GCP points obtained by the PS-InSAR in the previous step are used as control points for orbit refining and re-leveling, and the residual constant phase and phase ramp are estimated and removed. Finally, after the first and second SBAS inversions, the atmospheric phase and residual phase slope are removed, and finally accurate mining area settlement results are obtained. The deformation rate of the mining area is shown in Fig.6, and the cumulative settlement results of the mining area are shown in Fig.7.

5.0 Mining area settlement analysis

It can be seen from Fig.7 that there are obvious subsidences in the southern and eastern parts of the mining area. The subsidence in the southern part is more serious, and the amount of subsidence and subsidence are wide, and it affects some areas outside the mining area. By analyzing Fig.6 and Fig.7, the cumulative deformation range is $-66.59\text{mm}\sim 3.54\text{mm}$, and the average deformation rate range is $-53.65\text{mm/a}\sim 4.92\text{mm/a}$. Beginning in 2019, the No.2 mining group began experimenting with pillarless sublevel caving mining, which caused its settlement to increase continuously, which was consistent with the InSAR results.

GNSS settlement monitoring was carried out in the severely subsided areas in the south, and the monitoring time points were 2019-04 and 2020-06. The locations of the monitoring points are shown in Fig.8. The numbering sequence is from small to large to west to east and north to south. The elevations and differences of the monitoring data are shown in Table 2.

Comparing the GNSS settlement monitoring results with the SBAS-InSAR settlement monitoring results, it is found that the SBAS-InSAR results are highly consistent with the GNSS results, which fully shows that the fusion of InSAR technology can correctly obtain the overall situation of the surface settlement of the mining area.

6.0 Conclusions

This paper uses the fusion of PS-InSAR and SBAS-InSAR technology to monitor the settlement of the mining area based on Sentinel-1A data, and obtains the overall annual average deformation rate and cumulative deformation of the mining area.

- (1) According to the deformation results, there are obvious subsidences in the south and east of the West Second Mining Area. The main subsidence is in

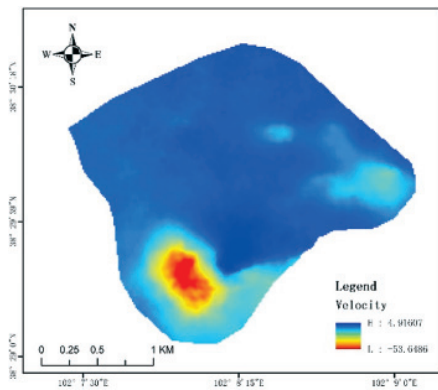


Fig.6: SBAS deformation rate

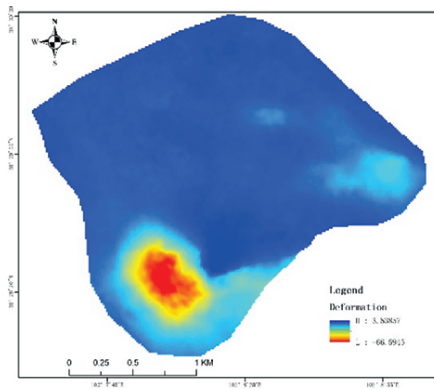


Fig.7: SBAS cumulative deformation

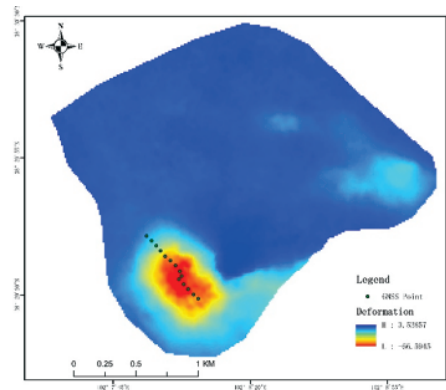


Fig.8: GNSS points

TABLE 2: GNSS MONITORING POINT VALUES (UNIT/MM)

	Deformation (GNSS)	Velocity (GNSS)	Deformation (InSAR)	Velocity (InSAR)	Difference (Deformation)	Difference (Velocity)
1.	-17.2	-14.7	-11.7	-9.6	-5.5	-5.1
2.	-18.6	-15.9	-15.6	-12.5	-3	-3.4
3.	-23.5	-19.3	-21.4	-16.9	-2.1	-2.4
4.	-38.6	-28.8	-30.1	-23.9	-8.5	-4.9
5.	-54.6	-43.2	-45.5	-36.4	-9.1	-6.8
6.	-55.8	-44.8	-48.4	-39	-7.4	-5.8
7.	-56.8	-46.3	-55.7	-46	-1.1	-0.3
8.	-57.1	-48.8	-62.6	-51.9	5.5	3.1
9.	-68.2	-54.9	-63.1	-51.9	-5.1	-3
10.	-63.8	-53.3	-60	-51.6	-3.8	-1.7
11.	-60	-50.2	-57.2	-46.4	-2.8	-3.8
12.	-60.8	-49.6	-58.1	-47.8	-2.7	-1.8
13.	-56.2	-48.2	-51.5	-44.5	-4.7	-3.7
14.	-53.4	-43.3	-45.7	-38.7	-7.7	-4.6

the south, with a large amount of subsidence and a wide subsidence area.

- (2) The maximum settlement of the mining area is 66mm, and the maximum settlement rate is 53mm/a.
- (3) The settlement results of the fusion InSAR are highly consistent with the GNSS settlement results, indicating that it is feasible to use the fusion InSAR technology to monitor the settlement of the mining area.

6.0 References

- [1] Xu Jun, Hu Jinshan, Kang Jianrong, et al. (2019): Monitoring and Analysis of Village Surface Subsidence in Mining Area Based on SBAS-InSAR[J]. *Metal Mine*, (10): 74-80. DOI:10.19614/j.cnki.jsks.201910012.
- [2] Zhou Wentao, Zhang Wenjun, Yang Yuanji, et al. (2021): A Combined Model Prediction Method for Surface Subsidence Monitoring in Mining Areas[J]. *Journal of Geodesy and Geodynamics*, 41(3):308-312. DOI: 10.14075/j.jgg.2021.03.016.
- [3] Xu Shuai, Wang Shangxiao, Niu Ruiqing. (2020): Identification of the Potential Landslide in Wushan-Fengjie in the Three Gorges Reservoir Area Based on InSAR Technology [J]. *Safety and Environmental Engineering*, 27(1):32-38. DOI:10.13578/j.cnki.issn.1671-1556.2020.01.006.
- [4] Du Xiaobei (2018): The Method of Screening the Hidden Geologic Hazard and Safety Evaluation in Mining Area Based on SBAS-InSAR [D]. Henan: Henan Polytechnic University.
- [5] GE Weili, LI Yuanjie, WANG Zhichao, Zhang Chunming, Yang Honglei. (2021): Spatial-Temporal Ground Deformation Study of Baotou Based on the PS-InSAR Method[J]. *Acta Geologica Sinica* (English Edition), 95(02):674-683.
- [6] Wu Jiang (2020): Application of PS-InSAR Technology in Urban Surface Subsidence Monitoring[J]. *Geomatics & Spatial Information Technology*, 43(12):208-210. DOI:10.3969/j.issn.1672-5867.2020.12.058.
- [7] Jiang Naiqi, Zuo Xiaoqing, Wang Zhihong, et al. (2020): Monitoring Land Settlement in the Main Urban Area of Kunming Based on PS-InSAR and SBAS Technology [J]. *Journal of Guizhou University (Natural Science)*, 2020, 37(4):72-78. DOI: 10.15958/j.cnki.gdxzb. 04.14.
- [8] Yang Yuanxin, Xu Wenxue. (2020): Subsidence monitoring of an airport based on PS-InSAR and SBAS-InSAR technology, 48(8):59-66.
- [9] Shi Gulin, Xu Liang, Zhang Xuanyu, et al. (2021): Monitoring time series deformation of Xishancun landslide with SBAS-InSAR, 46(2): 93-98, 105.
- [10] Irfan Ahmed Soomro, Fan Yubin, Guo Weina, et al. (2021): Surface subsidence monitoring in Juye coalfield based on SBAS-InSAR technology [J]. *Chinese High Technology Letters*, 31(3):333-340. DOI:10.3772/j.issn.1002-0470.2021.03.014.
- [11] Zhao Xijiang, Wang Bin, Zhang Zaiyan (2019): Monitoring and analysis of surface subsidence in Hegang mining area using SBAS-InSAR technology [J]. *Journal of Heilongjiang University of Science and Technology*, 29(1): 66-70. DOI:10.3969/j.issn.2095-7262.2019.01.012.
- [12] Wang Shangxiao, Niu Ruiqing, XU Shuai, et al. (2020): Landslide extraction in Wushan County based on SBAS technology [J]. *Yangtze River*, 51(8): 130-134, 146. DOI:10.16232/j.cnki.1001-4179, 08.023.